WAPD-TM-1350
DOE RESEARCH AND
DEVELOPMENT REPORT

FISSION GAS RELEASE FROM THO_2 AND THO_2-UO_2 FUELS

(LWBR Development Program)

AUGUST 1978

CONTRACT EY-76-C-11-0014

BETTIS ATOMIC POWER LABORATORY
WEST MIFFLIN, PENNSYLVANIA

Operated for the U. S. Department of Energy
WESTINGHOUSE ELECTRIC CORPORATION

DISCLAIMER

FISSION GAS RELEASE FROM ThO_2 AND ThO_2-UO_2 FUELS
(LWBR Development Program)

I. Goldberg
G. L. Spahr
L. S. White
L. A. Waldman
J. F. Giovengo
P. L. Pfennigwerth
J. Sherman

August 1978

Contract: EY-76-C-11-0014

Printed in the United States of America
Available from
National Technical Information Service
U. S. Department of Commerce
5285 Port Royal Road
Springfield, Va. 22161

NOTE

This document is an interim memorandum prepared primarily for internal reference and does not represent a final expression of the opinion of Westinghouse. When this memorandum is distributed externally, it is with the express understanding that Westinghouse makes no representation as to completeness, accuracy, or usability of information contained therein.

BETTIS ATOMIC POWER LABORATORY
WEST MIFFLIN, PENNSYLVANIA

Operated for the U. S. Department of Energy
BY WESTINGHOUSE ELECTRIC CORPORATION

FOREWORD

The Shippingport Atomic Power Station located in Shippingport, Pennsylvania was the first large-scale, central-station nuclear power plant in the United States and the first plant of such size in the world operated solely to produce electric power. This project was started in 1953 to confirm the practical application of nuclear power for large-scale electric power generation. It has provided much of the technology being used for design and operation of the commercial, central-station nuclear power plants now in use.

Subsequent to development and successful operation of the Pressurized Water Reactor in the DOE-owned reactor plant at the Shippingport Atomic Power Station, the Atomic Energy Commission in 1965 undertook a research and development program to design and build a Light Water Breeder Reactor core for operation in the Shippingport Station. In 1976, with fabrication of the Light Water Breeder Reactor (LWBR) nearing completion the Energy Research and Development Administration established the Advanced Water Breeder Applications program (AWBA) to develop and disseminate technical information which would assist U.S. industry in evaluating the LWBR-concept. All three of these reactor development projects have been administered by the Division of Naval Reactors with the goal of developing practical improvements in the utilization of nuclear fuel resources for generation of electrical energy using water-cooled nuclear reactors.

The objective of the Light Water Breeder Reactor project has been to develop a technology that would significantly improve the utilization of the nation's nuclear fuel resources employing the well-established water reactor technology. To achieve this objective, work has been directed toward analysis, design, component tests, and fabrication of a water-cooled, thorium oxide fuel cycle breeder reactor to install and operate at the Shippingport Station. Operation of the LWBR core in the Shippingport Station started in the Fall of 1977 and is expected to be completed in about 3 to 4 years. Then the fissionable fuel inventory of the core will be measured. This effort, when completed in about 2 to 3 years after completion of LWBR core operation, is expected to confirm that breeding actually took place.

The Advanced Water Breeder Applications (AWBA) project was initiated to develop and disseminate technical information that will assist U.S. industry in evaluating the LWBR concept for commercial-scale applications. The project will explore some of the problems that would be faced by industry in adapting technology confirmed in the LWBR program. Information to be developed includes concepts for commercial-scale prebreeder cores which will produce uranium-233 for light water breeder cores while producing electric power, improvements for breeder cores based on the technology developed to fabricate and operate the Shippingport LWBR core, and other information and technology to aid in evaluating commercial-scale application of the LWBR concept.

Technical information developed under the Shippingport, LWBR, and AWBA projects has been and will continue to be published in technical memoranda, one of which is this present report.

TABLE OF CONTENTS

LIST OF TABLES

LIST OF FIGURES

Fission gas release data are presented from 51 fuel rods irradiated as part of the LWBR irradiations test program. The fuel rods were Zircaloy-4 clad and contained ThO_2 or ThO_2-UO_2 fuel pellets, with UO_2 compositions ranging from 2.0 to 24.7 weight percent and fuel densities ranging from 77.8 to 98.7 percent of theoretical. Rod diameters ranged from 0.25 to 0.71 inches and fuel active lengths ranged from 3 to 84 inches. Peak linear power outputs ranged from 2 to 22 kw/ft for peak fuel burnups up to 56,000 MWD/MTM. Measured fission gas release was quite low, ranging from 0.1 to 5.2 percent. Fission gas release was higher at higher temperature and burnup and was lower at higher initial fuel density. No sensitivity to UO_2 composition was evidenced. A calculational model is described which includes terms to represent fission gas release as a function of temperature, using a diffusion model, and as a function of density to account for release due to knockout and recoil at free surfaces. The model is developed on both a best estimate and bounding basis.

FISSION GAS RELEASE FROM THO_2 AND THO_2-UO_2 FUELS
(LWBR Development Program)

I. Goldberg
G. L. Spahr
L. S. White
L. A. Waldman
J. F. Giovengo
P. L. Pfennigwerth
J. Sherman

I. INTRODUCTION

The amount of fission gases released from oxide fuel pellets during irradiation of fuel rods in power reactors is important to reactor design primarily in two design areas. First, release of fission gases from the fuel to the internal rod compartment results in an increase in rod internal pressure with increasing burnup. The higher internal pressure increases proximity to material property limits for a postulated loss of coolant accident (LOCA), during which fuel rod cladding can potentially experience high temperatures, resulting in loss of strength and more susceptibility to swelling and rupture. Second, since fission

gases (primarily xenon and krypton) have much lower thermal conductivity than the initial fill gas (typically helium or argon) used in light-water reactor fuel rods, more fission gas release can result in higher operating fuel temperatures due to the degraded heat transfer in the fuel-cladding gap. Such a mechanism has been suggested as a contributor to rod failures in the Maine Yankee reactor (Reference 1).

During the past 20 years of commercial nuclear power generation, a large data base has been accumulated on fission gas release for UO_2 fuel. However, prior to this report, very little information has been published on fission gas release from ThO_2 and ThO_2-UO_2 fuel.

This report presents (1) data on fission gas release from thoria and thoria-urania fuels obtained from 51 fuel rods irradiated as part of the LWBR Irradiations Test Program, and (2) comparisons of the measurements to a calculational model used in performance assessments. Dimensional, material characteristics, and environmental history of the test fuel rods are described in Section III. The fission gas release measurements are presented in Section IV along with a description of the measurement procedures and an assessment of measurement uncertainty. In Section V, the calculational model is described and the results of application of the model are compared to the measurements.

II. SUMMARY

Fuel rods in the LWBR Irradiation Test Program were Zircaloy-4 clad, non-pressurized (one atmosphere of helium, initial fill), and contained ThO_2 or ThO_2-UO_2 fuel pellets. Fuel densities ranged from 77.8 to 98.7 of theoretical, with over 80 percent of the test rods containing fuel 95 percent of theoretical density or greater. UO_2 composition in thoria-urania fuel pellets ranged from 2.0 to 24.7 weight percent. Fuel rod cladding was either recrystallized or stress relief annealed after fabrication. Rod diameters ranged from approximately 0.25 to 0.71 inch. Active (in-core) fuel pellet stack lengths were 3 to 7 inches in short rods and 30 to 84 inches in long rods. Peak linear power

outputs in 47 of the 51 rods ranged from 2 to 15 KW/ft with a maximum of 22 KW/ft for the 4 rods above 15 KW/ft. Peak fuel burnups ranged from about 1,000 to 56,000 MWD/MTM*, with peak centerline fuel temperatures of about 2,000 to 4,000°F.

Measured fission gas release (measurement uncertainty of plus or minus 8 percent of nominal) was generally low, ranging from less than 0.1 to 5.2 percent of the fission gases theoretically produced by fissioning. Gas release was predominantly below 2 percent for high density (95 percent theoretical or greater) fuels. Fission gas release was higher at higher temperatures, higher burnup and lower density. No sensitivity to UO_2 composition was observed.

A calculational model is presented which includes terms to represent fission gas release at both high temperatures (assuming a gas bubble diffusion model) and low temperatures (based on a recoil plus knockout mechanism). The high temperature term accounts for migrating gas bubbles which are released from the fuel due to intersection with a surface (e.g., cracks or open pores). Depending on specific fuel properties and burnup, critical temperatures for release of bubbles from dislocations and grain boundaries are calculated.

The low temperature term is adapted from a model which assumes that fission gas is released by recoil and knockout at free surfaces. Pellet density initially serves as a measure of free surface area, which increases with burnup (presumably due to fuel cracking). The model is developed on both a best estimate and bounding basis.

Gas release for long rods which experience non-uniform power profiles is calculated in several axial segments (using average power generation for each segment) and integrated along rod length. The best-estimate model fits through the middle of the scattered data. All data are conservatively bounded by the bounding model.

III. DESCRIPTION OF TEST FUEL RODS

A. Rod Characteristics

Test fuel rods from the LWBR development program were Zircaloy-4 clad, non-pressurized (one atmosphere of helium, initial fill) and contained ThO_2 or ThO_2-UO_2 fuel pellets. Rod characteristics are summarized in Table 1 for the

*MWD/MTM = Megawatt-days per metric tonne of metal (uranium + thorium).

51 rods for which fission gas release data have been obtained. The table is composed of 3 groups of rods classified by fuel type (100 percent ThO_2, ThO_2 + $U^{233}O_2$ and ThO_2 + $U^{235}O_2$).

Fuel characteristics given for each rod are composition, pellet density, pellet dimensions, and in-core fuel pellet stack length. Fuel compositions ranged from pure thoria to about 25 w/o UO_2. Fuel densities were generally 95 to 98 percent theoretical oxide density (10.0 gms/cc-ThO_2 and 10.24 gms/cc-ThO_2 + 25 w/o UO_2). Nominal fuel pellet dimensions are given, including endface geometry (flat or dished, with 4 to 22 mil dish depth). Fuel pellet diameters were 0.21 to 0.65 inch, with length/diameter ratios of 1.0 to 3.0. In-core fuel pellet stack length ranged from about 3 inches to 7 inches in short rods and from 30 inches to 84 inches in long rods.

Cladding heat treatment (RXA-recrystallization anneal or SRA-stress relief anneal), outside diameter, and diameter to wall thickness ratio are given for each rod. Rod diameters ranged from approximately 0.25 to 0.71 inch, with cladding OD/t ratios of 12 to 25. As-fabricated fuel-cladding diametral gaps were 0.002 to 0.010 inch. Fuel-cladding diametral gaps (no direct contact) are a source of thermal impedance and lead to higher fuel temperatures and greater gas release. Cladding OD/t and heat treatment affect the rate of creep down of the cladding diameter (under external pressure) and thereby the fuel-cladding diametral gap and gas release.

B. Rod Operating Parameters

Test fuel rods in the LWBR development program were operated in three different test reactors: (1) the Engineering Test Reactor (ETR) and (2) the advanced Test Reactor (ATR), both at the National Testing Station in Idaho, and (3) the National Test Reactor-Experimental (NRX) at Chalk River Nuclear Laboratory in Ontario, Canada. In-pile operating times ranged from less than 1000 to about 20,000 hours under nominal coolant conditions of 2000 psi and 550°F. Individual rod operating parameters are summarized in Table 2.

Peak and average axial linear power and fuel burnup are reported for each rod. Axial average values are equal to peak values for short rods, but are approximately 0.6 to 0.9 times the peak values for long rods. Figures 1 to 4

show peak power-burnup histories for four rods typical of those tested. Peak linear power of most rods ranged from 2 to 15 kw/ft with four of the 51 rods higher than 15 kw/ft up to a maximum of 22 kw/ft and peak burnup from about 1,000 to 56,000 MWD/MTM.

Peak values (axial position and operating history) of fuel temperatures* at the rod centerline and pellet surface were calculated using the CYGRO/FIGRO computer programs (References 2 and 3). Centerline fuel temperatures at the peak axial power locations ranged from less than 2000 to over 4000°F and fuel pellet surface temperatures ranged from about 800 to 1800°F. These temperatures are low relative to the thoria-base oxide melting temperatures (about 5900°F) so that no significant fuel redistributions due to pellet coring or melting were expected. Such conditions have not been observed in the test rods examined to date.

The ThO_2 dislocation release temperature (for release of gas bubbles from dislocations) was also calculated for each rod, assuming peak conditions and using the model by Warner (Reference 4). This temperature provides a measure of fractional fuel pellet volume for intermediate-high temperature fission gas release as discussed in Section V.A.1 below. The ThO_2 dislocation release temperatures range from about 2630 to 2930°F.

IV. FISSION GAS RELEASE MEASUREMENTS

In the following sections, IV.A through IV.C, remote measurement procedures and techniques and calculational procedures are presented for the determination of percent fission gas release data from irradiated test fuel rods. Measurement and calculational uncertainties also are presented and discussed. The data are presented in tabular and graphical form in Table 2 and Figure 8, respectively.

A. Measurement Procedures

After a delay time sufficient to allow short lived fission products (especially iodine) to decay, irradiated test rods selected for fission gas measurements are punctured (through-cladding hole drilled) and the free internal gases collected. Fission gas measurements are obtained by the following procedure:

1. Rod is punctured while in an evacuated chamber.
2. All gas released from the rod is collected in several sealed bulbs (including an initial and final bulb for background atmosphere in the evacuated chamber).

---

*Time averaged temperatures are approximately 80 percent of peak temperatures.

3. Each bulb is measured for pressure, temperature, and total gas volume.
4. Mass spectrometric analyses are run on each bulb and the percent Xe, Kr, He, O_2, N_2, H_2, H_2O, and CO_2 reported. (Not all these gases are analyzed for every rod.)
5. The number of fission gas atoms (Xe + Kr) are calculated for each bulb using the volume percent from mass spectrometry, the pressure, and temperature and total volume of each bulb, and the ideal gas law.
6. The number of gas atoms produced in the fuel are calculated from the average rod burnup (fissions/cc), the fuel volume, and the fission yield (0.33 atom Xe + Kr gases per U^{233} fission or 0.30 atom Xe + Kr gases per U^{235} fission).
7. Percent fission gas released is calculated from the number of fission gas atoms collected out of the punctured rod divided by the number of gas atoms calculated to have been produced.

B. Uncertainties

There are several sources of uncertainty or error in determining the percent fission gas release. These uncertainties are of 3 major types: (1) efficiency of gas collection, (2) uncertainty in mass spectrometry measurements, and (3) uncertainties in the actual fuel burnup and fission product yields.

These uncertainties are discussed below:

1. Gas Collection Efficiency

The efficiency of fission gas collection from a punctured fuel rod is evaluated relative to collection of the helium fill gas and relative amounts of Xe and Kr. Relative average yields of the 2 fission product gases, Kr and Xe, were 15 percent Kr (±1.2 percent) plus 85 percent Xe (±1.2 percent) for U^{235} fissioning and 19 percent Kr (±1.3 percent) plus 81 percent Xe (±1.3 percent) for U^{233} fissioning. The uncertainties are 1 sigma values. These measured Kr and Xe yields are in good agreement with theoretical yields. Helium recovery measurements from irradiation test rods are summarized in Table 3. Irradiation test rods were filled with helium at approximately 1 atmosphere pressure to provide an inert atmosphere with high thermal conductivity. Since variations from 1 atmosphere pressure were considered to be allowable in meeting these objectives, the initial gas pressure in many test rods was not measured. In the case of some test rods, however, a Bourdon gage indicating a zero (0) dial reading at atmospheric pressure with a scale of ±1 atmosphere was used to establish the helium pressure in the rods within a range of 0.95 to 1.05 atmospheres. Six of

these rods (79-610, 613, 617, 623, 631, and 632) were punctured for fission gas collection after irradiation. Measurements of helium in the rod atmosphere showed a 1 sigma variation of ±0.05 atmospheres with a mean value of 0.97 atmospheres and a range of 0.92 to 1.07 atmospheres. This range represents about a ±7 percent variation from the target pressure of 1 atmosphere and is considered to be the variation in the weld box pressure during rod fabrication. It is noted that the additional helium produced as a result of ternary fissioning is considered to be negligible in its effect on collection efficiency for the fission gas releases of Table 2. In addition to these measurements performed directly on punctured fuel rods, an unirradiated dummy rod filled with helium at a gage pressure of 1 ± 0.02 atmospheres was punctured for helium collection. In this case, the collected helium corresponded to 1.02 atmospheres internal pressure at original loading conditions, thus indicating essentially complete gas collection. These results for the unirradiated dummy rod together with the test rod fill gas pressure data discussed above indicate complete gas collection. It is concluded that 100 percent efficiency in collection of fission gases may be assumed.

2. Fission Gas Atom Measurement

An overall accuracy has been assessed for the measured pressure, volume, and temperature and for the mass spectrometer analysis to estimate the measurement accuracy for the number of fission gas atoms collected. Standard samples of fission gases were prepared by mixing known quantities of Xe + Kr in a sample bulb which was certified by mass spectrometry and gas chromotography measurements. These standard sample bulbs were introduced into the fission gas mass spectrometer system for measurement of the overall system accuracy. The ambient temperature was measured by a thermometer, pressure was measured by a capacitance manometer, and the sample bulb volumes were calibrated by weighing the volume of water which filled these bulbs at a measured temperature. The two sigma accuracy of the mass spectrometric analyses including the pressure, volume, and temperature measurements is ±4 percent.

3. Calculation of Fission Gas Produced

The above errors pertain to uncertainties for measurements of the amount of fission gases released from the fuel. Additional uncertainty exists, in the

calculation of percent gas release, for the amount of fission gas produced which is dependent on the rod average burnup and fission yield (i.e., gas atoms produced = burnup x gas atoms per fission).

A 2 sigma error of ±6 percent has been established for burnup measurements. In addition, a bias of about -10 percent in the rod average burnup computed from the test reactor axial profile is shown by burnup measurements on several long test rods (i.e., 79-439, 79-576, and 79-605). The bias on average burnup based on the core axial profile is attributed to a change in the test axial power profile as a result of non-uniform burnup of the rods in the axial direction. The effect of this axial variation in test burnup is to flatten the test power shape. This produces relatively higher axial factors for the lower power test positions. As a result of this bias, the average test burnup and hence the calculated amount of fission gas produced is increased by 10 percent. Thus, the percent gas release (i.e., measured/produced x 100 percent) for long test rods is potentially reduced 10 percent below the values presented in Table 2.

A 2 sigma measurement uncertainty of ±4 percent is assigned to the fission yield of xenon and krypton fission gases by the data compiled in Reference 13.

4. Combined Uncertainty for Fission Gas Release

The overall 2 sigma uncertainty in the fission gas release is given (from analysis of variance) by:

$$2\sigma = \left[(2\sigma_1)^2 + (2\sigma_2)^2 + (2\sigma_3)^2 \right]^{1/2}$$

assuming independent errors where

$2\sigma_1$ = fission gas measurement uncertainty

$2\sigma_2$ = burnup measurement uncertainty (not including the bias discussed above)

$2\sigma_3$ = fission yield uncertainty.

Hence,

$$2\sigma = \left[4^2 + 6^2 + 4^2 \right]^{1/2} = \pm 8 \text{ percent}$$

of the measured percent gas release.

For example, the percent gas release for a measured 1 percent release would be 0.92 to 1.08 percent. If the 10 percent relative bias in rod average burnup is included, the measured 1 percent release would be 1 percent + (-0.1 ± 0.08) or 0.9 percent ± 0.08 percent = 0.82 to 0.98 percent.

C. Data

Fission gas release data were obtained on 51 irradiated test rods and percent fission gas release computed from calculations of the fission gas produced in the fuel, using average burnup in long rods based on the test reactor axial profile as shown, for example, in Figure 5. The data on percent of fission gas release are presented in Table 2.

Due to the scatter of the fission gas release data presented in Table 2, a correction factor was established to account for the effect of sintered fuel pellet density on the fission gas release. This factor was assumed to take the form:

$$R_n = \left(\frac{\%\ TD}{100}\right)^u R_m$$

where

R_n = normalized gas release
R_m = measured gas release
TD = theoretical density
u = a constant.

The measured gas release data were used to determine the value of the exponent, u, as follows:

1. The measured gas release data were plotted as a function of the average burnup (in 10^{20} fiss/cc).
2. A best fit curve correlating gas release and burnup was established.
3. The necessary correction to fit the exceptionally high gas release data point from low density test rod 79-318 to this curve was determined using the above equation. The resulting value of u, 10.25, was used to normalize the gas release data for all the samples.

The normalized gas releases are presented in Table 2 and in Figure 6 where the normalized gas release is plotted versus rod average burnup. Open symbols in Figure 6 represent those rods in which calculated fuel centerline temperatures were less than the dislocation release temperature, discussed below in Section V.A.1. Solid symbols in Figure 6 represent those rods in which calculated

fuel centerline temperatures were greater than the dislocation release temperature. This normalization does tend to reduce data scatter by an approximate factor of 2. The wide data scatter for similar environment is unexplained at present. However, gas release values are quite low for the ThO_2 and ThO_2-UO_2 fuel, and variations in pellet cracking patterns may account for the scatter. Note that normalized gas release tends to increase with increased operating fuel temperature and burnup.

V. COMPARISON OF MEASUREMENT DATA TO CALCULATIONAL MODEL

A. Description of Calculational Model

A number of investigators (References 4, 5, 6, 7, 8, and 12) have proposed models for fission gas release from oxide fuels. These models have in common the assignment of fission gas release fractions to several temperature intervals, e.g., Lewis (Reference 5) selects 1000°C, 1300°C, and 1600°C as defining the intervals. Beyer and Hann (Reference 6) select 1200°C, 1400°C, and 1700°C. In these models, the fission gas release fraction increases with increasing temperature. At low temperatures (below about 1000°C), most models include a term that allows for some fractional release due to fission product recoil and knockout at free surfaces. Warner's model (Reference 4) relates low temperature fission gas release linearly to irradiation time. Bellamy and Rich (Reference 8) proposed a low temperature fission gas release model which relates gas release to fuel initial density (as a measure of free surface area) and burnup (as a measure of the increase in fuel fracture surfaces with increasing irradiation).

The model selected to correlate the fission gas release measurements reported above combines the high temperature model of Warner (Reference 4) with a modified low temperature model derived from Bellamy and Rich (Reference 8).

1. High Temperature Fission Gas Release Model

In Warner's model, fission gas atoms are assumed to nucleate in small bubbles that migrate up the thermal gradient to dislocation lines. At a dislocation, coalescence with pre-existing bubbles occurs and bubble size is increased. With time, a critical bubble size is reached for pull-off from the dislocation and the bubble again migrates up the thermal gradient. A fraction of these bubbles are released by intersection with a free surface. The remaining bubbles continue to migrate until intersection with a grain boundary. At a grain boundary, coalescence with existing bubbles occurs, increasing bubble size, until

the critical grain boundary pull-off size is reached. On pull-off from the grain boundary, the bubble is again free to migrate up the thermal gradient. Some bubbles released from both dislocation lines and grain boundaries, after traveling some distance, intersect with free surfaces (such as cracks or pores) and are released from the fuel matrix.

A critical temperature for pull-off from dislocation lines and grain boundaries can be calculated (Reference 4) from critical bubble radii:

$$\text{for dislocation lines, } r_d = \sqrt[3]{\frac{\Omega\, T\, \mu\, b^2\, F}{2\pi\, Q_s^*\, dT/dX}}$$

$$\text{for grain boundaries, } r_{gb} = \sqrt{\frac{\Omega\, \gamma_{gb}\, T\, F}{2\, Q_s^*\, dT/dX}}$$

where

r_d = critical bubble radius for pull-off from dislocation lines (cm)

r_{gb} = critical bubble radius for pull-off from grain boundaries (cm)

Ω = molecular volume transferred per diffusing species (cm^3)

T = temperature (°K)

μ = shear modulus (dyne/cm^2)

b = Burger's vector of the dislocation (cm)

μb^2 = dislocation line tension (10^{-4} dyne)

γ_{gb} = grain boundary surface tension (dyne/cm)

Q_s^* = heat of transport for surface diffusion (cal/mole)

dT/dX = fuel thermal gradient (°K/cm)

F = unit conversion factor = 1.4387×10^{16} cal/dyne-mole-cm.

The bubble velocity is computed using the following equation:

$$V = \frac{3 D_s\, \upsilon_s\, \Omega\, Q_s^*}{rK\, T^2\, N} \frac{dT}{dX}$$

where

V = bubble velocity (cm/sec)

D_s = surface diffusion coefficient = $D_o e^{-Qs/RT}$ (cm^2/sec)

Q_s = activation energy for surface self-diffusion (cal/mole)

R = universal gas constant = 1.986 cal/mole - °K

υ_s = concentration of rate controlling diffusing species = $\Omega^{-2/3}$ ($1/cm^2$)

r = bubble radius (cm)

K = Boltzmann's constant = 3.2982×10^{-24} cal/°K

N = Avogadro's number = 6.0222×10^{23}/mole.

Assuming that the bubble radius during migration is unchanged from the critical radius at pull-off and that its velocity is unchanged during migration, the time the bubble takes to migrate a fixed distance can be calculated as a function of bubble temperature. This assumption introduces some inaccuracy since the bubble radius increases as it migrates up the gradient, thus tending to decrease velocity. However, as it migrates to a region of higher temperature, its velocity tends to increase. Overall, the temperature effect should nullify the radius effect. Thus the inaccuracy introduced by the above assumptions is small.

Migration distances of 10 microns for release from dislocation lines (the order of the grain size) and 0.1 cm for release from grain boundaries are assumed in this analysis. A temperature gradient of 10^3°C/cm is assumed, also. A value of 300 dyne/cm is used for grain boundary surface tension. The other constants used in this analysis are listed below

Parameter	ThO_2*	UO_2
Ω	4.38×10^{-23} cm^3	4.09×10^{-23} cm^3
$Q_s = Q_s^*$	1.26×10^5 cal/mole	9.507×10^4 cal/mole
D_o	4.4×10^5 cm^2/sec	10^4 cm^2/sec

The calculated critical (release) temperatures are shown in Figure 7. As indicated, release temperatures (from both dislocations and grain boundaries) for ThO_2 are higher than for UO_2. This suggests that, at equivalent temperatures, UO_2 fuel releases a larger fractional amount of fission gas than does ThO_2.

The fractional amount of fission gas released can be calculated using the critical release temperatures shown in Figure 7 and calculated radial temperature profiles for the fuel. Let R_H equal the percent fission gas released at high temperature, V_d equal the fraction of total fuel volume at temperatures above T_d (the critical release temperature from dislocations) but below T_{gb} (the critical release temperature from grain boundaries) and V_{gb} equal the fraction of total fuel volume above T_{gb}. Then,

$$R_H = A\, V_{gb} + B\, V_d \quad ,$$

*ThO_2 values were used for both ThO_2 and ThO_2-UO_2.

where A and B are fitted coefficients.

For a parabolic radial temperature profile,

$$V_{gb} = \frac{T_c - T_{gb}}{T_c - T_s} \text{ and } V_d = \frac{T_{gb} - T_d}{T_c - T_s}$$

where T_c = fuel center temperature and T_s = fuel outer surface temperature. Thus,

$$R_H = \frac{A(T_c - T_{gb}) + B(T_{gb} - T_d)}{T_c - T_s}$$

Calculated values of the dislocation release temperature (T_d) for thoria base fuel using ThO_2 properties for both ThO_2 and ThO_2-UO_2 fuel are given in Table 2 for the test rods. Grain boundary release temperatures are not given since, in these fuels, the higher temperature contribution was insignificant.

2. Low Temperature Fission Gas Release Model

The low temperature release model of Bellamy and Rich (Reference 8) relates gas release to a measure of fuel free surfaces (including cracks and pores), which is dependent on initial fuel density and burnup. Beyer and Hann (Reference 6) present data indicating an exponential relationship between fuel free surface area and burnup for fuel at high initial density (98 percent of theoretical), and a power law relationship between fuel free surface area and initial density. However, for burnups less than about 12 x 10^{20} fissions/cc (~45,000 MWD/MTM) a linear dependence results in an adequate fit to the data reported above. The resulting low temperature release model is given by:

$$R_L = \left(\frac{100}{\rho}\right)^u (V + WD)$$

where

R_L = low temperature fission gas release (percent)
ρ = fuel initial density (percent of theoretical)
D = burnup (10^{20} fissions per cubic centimeter of fuel)
and u, V and W are fitted constants.

B. Model for Fission Gas Release in Thoria Base Oxide Fuels

A model that incorporates both the high and low temperature gas release mechanisms of the two models described above would be the most suitable for

predicting gas release from thoria base oxide fuels. As described below, the proposed model was applied to the fission gas release measurements reported in Section III to obtain constants for the high and low temperature release terms. Both best fit and bounding values for the constants were obtained using the values for burnup and temperature presented in Table 2. A number of test rods operated at fuel temperatures below the temperature for release from dislocations and from grain boundaries. Data from these rods were used to obtain values for the constants in the low temperature release term, as shown in Figure 6. Then, using the resulting calculated values for low temperature release and the data from rods that operated at higher temperatures, values for the constants in the high temperature release term were obtained. Since only a few of the test rods operated at temperatures above T_{gb}, little sensitivity to the constant B was calculated for fission gas release. Thus, A and B were assigned the same value. The resulting models for both best estimate and bounding values are:

Best Estimate

$$R = 5\left(\frac{T_c - T_d}{T_c - T_s}\right) + \left(0.05D\right)\left(\frac{100}{\rho}\right)^{10.25}$$

Bounding

$$R = 15\left(\frac{T_c - T_d}{T_c - T_s}\right) + \left(0.5 + 0.1D\right)\left(\frac{100}{\rho}\right)^{10.25}$$

A comparison of the measured fission gas release data to the calculational model is presented in Figure 8. Figure 8a displays the best estimate fit while Figure 8b shows the comparison to the bounding model. Calculated values for long rods which experience a non-uniform power profile were obtained by calculating fission gas release appropriate to the highest temperature calculated during irradiation life at several axial locations along the length of the rod (using the power generation appropriate to each location, per Figure 5) and integrating along the length of the rod. Both long (30 to 100 inches) and short (4 to 11 inches) rod data are presented in Figure 8. As indicated, the best estimate model gives a good average fit to the data, while all data are conservatively upper bounded by the bounding model.

VI. CONCLUSION

Within the range of parameters tested for 51 fuel rods containing ThO_2 or ThO_2-UO_2 fuel, the following is concluded:

1. Fission gas release is greater at higher fuel temperatures and burnups. These effects can be satisfactorily predicted by a model which accounts for gas bubble coalescence and release from grain boundaries and dislocations.
2. Higher initial fuel density results in significantly less fission gas release. This effect can be satisfactorily predicted by a model which accounts for release due to recoil and knockout of gas bubbles at free surfaces.
3. No sensitivity to UO_2 composition or rod diameter was observed.

The values of fission gas release obtained from ThO_2 and ThO_2-UO_2 fuel for 51 fuel rods are quite low, less than about 3 **percent** release for high density (95 percent TD or greater) fuel. These data support other performance advantages exhibited by ThO_2-based fuels relative to UO_2 fuels. For example, compared to UO_2, ThO_2 has a higher melting temperature (Reference 9), higher thermal conductivity (Reference 10), and is more corrosion resistant when exposed to oxygenated reactor coolant (Reference 11). Thus, ThO_2-based fuel rods could be designed for higher power ratings than UO_2 fuel rods for equivalent fuel temperature or margin to melting.

Peak power ratings (from Table 2) of 82 percent of the test rods are in the range of about 6 to 14 KW/ft. The peak power rating generally occurred at the beginning or early in the test life, with typically a 40-50 percent decrease in power rating throughout the test life. The test data reported here would support low expected fission gas release for high density ThO_2 and ThO_2-UO_2 fuels with initial peak power ratings up to at least 14 KW/ft in rods operated at generally decreasing power rating throughout life.

The calculational model proposed for thoria base fuels satisfactorily bounds the measurements and thus is suitably conservative for use in performance assessments. Improved agreement might be obtained by including explicitly in the model representations of grain restructuring, fission gas resolution effects, fuel crack formation, and the effect of time varying temperature. However, there are insufficient data at temperatures above 4000°F to assess such representations quantitatively.

VII. ACKNOWLEDGMENTS

The contributions of Messrs. J. T. Engel, R. C. Hoffman, L. R. Lynam, D. A. Mertz and C. D. Sphar in examining specimens, performing analyses and reporting results are gratefully acknowleged. The authors also thank H. R. Warner, C. C. Dollins and R. A. Frederickson for helpful discussions.

VIII. REFERENCES

1. N. Fuhrman, V. Pasupathi, and T. E. Hollowell, "Joint CE/EPRI Fuel Performance Evaluation Program, Task C, Evaluation of Fuel Rod Performance in Maine Yankee Core I, "CENPD-221, December 1975.
2. J. B. Newman, J. F. Giovengo, and L. P. Comden, "The CYGRO-4 Fuel Rod Analysis Computer Program," WAPD-TM-1300, July 1977.
3. I. Goldberg, "A Procedure for Calculation of Steady-State Temperature in Zircaloy-Clad Bulk Oxide Fuel Elements Using the FIGRO Computer Program," WAPD-TM-757, November 1969.
4. H. R. Warner, "Release of Fission Gases from Oxide Fuels (LWBR Development Program)," WAPD-TM-805, July 1969.
5. W. B. Lewis, "Engineering for the Fission Gas in UO_2 Fuel," Nuclear Applications, Vol. 2, April 1966, Pages 171-182.
6. C. E. Beyer and C. R. Hann, "Prediction of Fission Gas Release From UO_2 Fuel," BNWL 1875, November 1974.
7. R. Hargreaves, D. A. Collins, "A Quantitative Model for Fission Gas Release and Swelling in Irradiated Uranium Dioxide," J. Br. Nucl. Energy Soc., Vol. 15, No. 4, October 1976, Pages 311-318.
8. R. G. Bellamy and J. B. Rich, "Grain Boundary Gas Release and Swelling in High Burnup Uranium Dioxide", J. Nucl. Mat. 33 (1969), Pages 64-78.
9. W. A. Lambertson, M. H. Mueller, and F. H. Bunzel, Jr., J. Am. Ceram. Soc. 36, 397-399 (1953)
10. R. M. Berman, T. S. Tully, J. Belle and I. Goldberg, "The Thermal Conductivity of Polycrystalline Thoria and Thoria-Urania Solid Solutions (LWBR Development Program)," WAPD-TM-908, December 1972.
11. J. M. Markowitz and J. C. Clayton, "Corrosion of Oxide Nuclear Fuels in High Temperature Water (LWBR Development Program)," WAPD-TM-909, February 1970.
12. C. C. Dollins and F. A. Nichols, "Swelling and Gas Release in UO_2 at Low and Intermediate Temperatures," J. Nucl. Mat. 66 (1977) Pages 143-157.

13. M. E. Meek and B. F. Rider, "Compilation of Fission Product Yields," Vallecitos Nuclear Center, NEDO-12154-1, 1974.

TABLE 1. SUMMARY OF FUEL ROD CHARACTERISTICS

	Rod Serial No.	Fuel: Composition (Wt. % UO_2 in ThO_2)	Fuel: Average Density (% Theoretical)	Fuel: Pellet Dimensions (in.) Diameter	Fuel: Pellet Dimensions (in.) Length	Fuel: Pellet Dimensions (in.) End Face Geom*	Fuel: In-Core Pellet Stack Length (in.)	Fuel-Clad Diam. Gap (mils)	Cladding: Rod Diam. (in.)	Cladding: OD/t Ratio**	Cladding: Heat Treatment†
A.	ThO_2 Fuel										
	81-39	0.0	77.8	0.241	0.25	Flat	3.3	1.3	0.287	17.5	RXA
	81-46	0.0	96.2	0.241	0.25	Dish	3.3	7.7	0.281	17.0	RXA
	81-53	0.0	96.3	0.241	0.25	Dish	3.3	3.9	9.277	17.3	RXA
	81-74	0.0	97.6	0.242	0.47	Dish	3.5	3.0	0.284	14.6	SRA
	81-76	0.0	98.7	0.242	0.47	Dish	3.5	3.0	0.284	14.6	SRA
	81-81	0.0	97.6	0.239	0.49	Dish	3.5	6.4	0.284	14.6	RXA
	81-85	0.0	93.5	0.238	0.49	Dish	3.5	6.9	0.284	14.6	SRA
B.	$ThO_2 + U^{233}O_2$ Fuel										
	79-439	6.6	96.0	0.210	0.42	Dish	30.0	4.9	0.255	13.3	RXA
	79-442	6.6	96.0	0.208	0.42	Dish	30.0	7.1	0.255	12.5	RXA
	79-445	6.6	96.0	0.210	0.42	Dish	30.0	4.8	0.255	13.2	RXA
	79-449	6.6	96.0	0.208	0.42	Dish	30.0	6.1	0.255	12.3	RXA
	79-455	6.6	96.0	0.208	0.42	Dish	30.0	7.0	0.255	12.4	RXA
	79-477	8.5	97.0	0.210	0.41	Dish	3.2	5.3	0.253	13.4	RXA
	79-481	8.5	98.0	0.206	0.41	Dish	3.2	8.8	0.253	13.4	RXA
C.	$ThO_2 + U^{235}O_2$ Fuel										
	79-318	7.7	86.2	0.219	0.23	Flat	3.2	2.3	0.264	12.6	SRA
	79-320	7.7	91.2	0.219	0.23	Flat	3.2	2.1	0.264	12.6	SRA
	79-349	20.0	95.0	0.652	0.23	Flat	3.2	4.0	0.716	23.9	SRA
	79-363	24.7	89.3	0.207	0.23	Flat	30.0	2.9	0.249	12.4	SRA
	79-382	20.3	90.1	0.208	0.40	Dish	3.2	2.0	0.248	12.9	RXA
	79-429	2.0	98.0	0.542	0.83	Dish	30.0	10.0	0.600	24.6	SRA
	79-467	3.4	98.1	0.547	0.60	Dish	84.0	4.9	0.600	25.0	SRA

*Dished ends have spherical segment cavities with depths of 4 to 22 mils and end lands have widths about 10 percent of the pellet diameter.

**Diameter to wall thickness ratio is a measure of cladding stability under external pressure.

†RXA = recrystallization anneal; SRA = stress relief anneal.

TABLE 1 (Cont)

Rod Serial No.	Fuel: Composition (Wt. % UO_2 in ThO_2)	Fuel: Average Density (% Theoretical)	Fuel: Pellet Dimensions (in.) Diameter	Length	End Face Geom*	Fuel: In-Core Pellet Stack Length (in.)	Fuel-Clad Diam. Gap (mils)	Cladding: Rod Diam. (in.)	Cladding: OD/t Ratio**	Cladding: Heat Treatment†
C. $ThO_2 + U^{235}O_2$ Fuel (Cont)										
79-478	11.4	97.2	0.206	0.41	Dish	3.2	9.2	0.253	13.4	RXA
79-500	22.6	97.9	0.210	0.47	Dish	84.0	5.4	0.250	14.7	RXA
79-501	22.6	97.9	0.206	0.47	Dish	84.0	8.7	0.251	13.9	RXA
79-506	17.1	95.3	0.462	0.93	Dish	36.0	6.9	0.527	18.0	SRA
79-509	17.1	96.8	0.464	0.65	Dish	36.0	5.4	0.523	19.7	SRA
79-513	17.1	95.6	0.504	0.75	Dish	15.0‡	6.1	0.568	20.1	SRA
79-514	17.1	95.6	0.507	0.87	Dish	15.0‡	4.0	0.568	19.7	SRA
79-522	17.1	98.7	0.466	0.77	Dish	36.0	4.2	0.522	20.0	SRA
79-551	8.4	94.8	0.455	0.68	Dish	6.6	2.7	0.508	19.7	SRA
79-570	2.8	97.8	0.507	1.01	Dish	30.0	3.8	0.568	19.9	SRA
79-572	2.8	98.2	0.507	0.76	Dish	30.0	3.7	0.569	19.6	SRA
79-573	2.8	92.7	0.503	0.77	Dish	30.0	7.8	0.568	19.6	SRA
79-575	3.1	97.6	0.548	0.82	Dish	84.0	4.0	0.612	20.1	SRA
79-576	3.1	97.5	0.545	0.82	Dish	84.0	7.1	0.613	20.2	SRA
79-586	2.8	93.0	0.503	0.77	Dish	30.0	7.7	0.567	20.2	SRA
79-588	5.7	97.3	0.247	0.58	Dish	6.9	9.8	0.301	13.6	RXA
79-590	5.7	97.4	0.247	0.58	Dish	6.9	10.0	0.301	13.6	RXA
79-591	5.7	97.3	0.247	0.58	Dish	6.9	9.8	0.301	13.6	RXA
79-602	19.2	96.5	0.252	0.60	Dish	84.0	5.6	0.300	14.0	RXA
79-603	19.2	95.5	0.248	0.72	Dish	84.0	8.8	0.300	13.8	RXA
79-605	19.2	96.4	0.248	0.60	Dish	84.0	8.8	0.301	13.6	RXA
79-608	19.2	97.5	0.251	0.72	Dish	84.0	5.8	0.301	13.6	RXA
79-610	4.5	97.2	0.250	0.74	Dish	35.0	8.7	0.305	13.2	RXA
79-613	4.5	96.6	0.250	0.74	Dish	35.0	8.5	0.306	12.9	RXA
79-617	4.5	97.2	0.249	0.75	Dish	35.0	10.3	0.303	13.8	RXA
79-623	4.5	97.2	0.250	0.74	Dish	35.0	8.6	0.301	14.3	RXA

*Dished ends have spherical segment cavities with depths of 4 to 22 mils and end lands have widths abouth 10 percent of the pellet diameter.

**Diameter to wall thickness ratio is a measure of cladding stability under external pressure.

†RXA = recrystallization anneal; SRA = stress relief anneal.

‡An additional 21 inches of thoria pellets is in the core region.

TABLE 1 (Cont)

Rod Serial No.	Fuel: Composition (Wt. % UO_2 in ThO_2)	Fuel: Average Density (% Theoretical)	Fuel: Pellet Dimensions (in.) Diameter	Fuel: Pellet Dimensions (in.) Length	Fuel: End Face Geom*	Fuel: In-Core Pellet Stack Length (in.)	Fuel-Clad Diam. Gap (mils)	Cladding: Rod Diam. (in.)	Cladding: OD/t Ratio**	Cladding: Heat Treatment†
C. $ThO_2 + U^{235}O_2$ Fuel (Cont)										
79-631	4.5	97.0	0.251	0.74	Dish	35.0	7.5	0.299	14.7	RXA
79-632	4.5	97.0	0.250	0.74	Dish	35.0	8.6	0.300	14.5	RXA
79-656	4.5	97.2	0.250	0.74	Dish	7.0	8.0	0.300	14.3	RXA
79-671	4.5	97.0	0.250	0.74	Dish	7.0	8.1	0.300	14.3	RXA

*Dished ends have spherical segment cavities with depths of 4 to 22 mils and end lands have widths about 10 percent of the pellet diameter.

**Diameter to wall thickness ratio is a measure of cladding stability under external pressure.

†RXA = recrystallization anneal; SRA = stress relief anneal.

TABLE 2. SUMMARY OF FUEL ROD OPERATING PARAMETERS AND FISSION GAS RELEASE

	Rod Serial No.	Time In-Pile (1000 Hours)	Linear Power (KW/ft) Peak	Linear Power (KW/ft) Ave.	U + Th Burnup (MWD/MTM) Peak	U + Th Burnup (MWD/MTM) Ave.	Peak Fuel Temp. (°F) Center	Peak Fuel Temp. (°F) Surface	ThO_2 Disl' cn. Release Temp., T_d (°F)	Fission Gas Release (%) Measured	Fission Gas Release (%) Normalized†
A.	ThO_2 Fuel										
	81-39	7.40	6.52	6.52	16,400	16,400	*	*	2,700	1.2	0.091
	81-46	10.38	9.06	9.06	38,000	38,000	2,544	1,200	2,670	0.2	0.134
	81-53	10.40	11.26	11.26	38,000	38,000	*	*	2,662	1.0	0.679
	81-74	4.75	8.72	8.72	4,800	4,800	*	*	2,980	0.5	0.370
	81-76	9.20	4.36	4.36	8,200	8,200	*	*	2,905	0.2	0.164
	81-81	2.55	2.18	2.18	900	900	*	*	2,805	0.1	0.078
	81-85	2.55	2.18	2.18	900	900	*	*	2,805	0.2	0.100
B.	$ThO_2 + U^{233}O_2$ Fuel										
	79-439	3.70	10.00	7.04	23,800	16,700	2,780	1,270	2,770	0.4	0.263
	79-442	8.54	10.35	7.24	45,300	31,700	3,310	1,520	2,685	0.5	0.329
	79-445	8.54	9.94	6.96	44,000	30,800	2,725	1,268	2,680	0.6	0.401
	79-449	8.54	10.12	7.07	45,300	31,700	3,125	1,430	2,685	0.5	0.329
	79-455	3.70	9.29	6.54	23,800	16,700	2,970	1,450	2,770	0.4	0.243
	79-477	11.00	8.12	8.12	52,100	52,100	2,206	**	2,660	2.3	1.683
	79-481	11.00	8.26	8.26	49,900	49,900	2,950	1,470	2,660	2.8	2.276
C.	$ThO_2 + U^{235}O_2$ Fuel										
	79-318	5.20	8.91	8.63	30,300	29,400	2,920	840	2,735	5.2	1.134
	79-320	4.70	7.98	7.98	24,400	24,417	2,320	870	2,740	2.0	0.236
	79-349	11.10	22.45	15.30	9,700	6,600	3,934	829	2,660	1.8	1.064
	79-363	3.80	10.45	7.35	27,500	18,500	*	*	2,762	0.3	0.094
	79-382	0.55	10.94	10.94	5,600	5,600	*	*	2,960	0.1	0.034
	79-429	4.44	13.67	9.94	4,800	3,500	3,525	1,525	2,750	0.1	0.049
	79-467	16.40	17.27	15.32	26,800	23,700	3,060	890	2,630	1.2	0.985
	79-478	11.00	7.94	7.94	50,600	50,600	2,900	1,500	2,660	2.6	1.942
	79-500	8.46	10.05	7.61	47,100	35,700	3,250	1,400	2,710	0.4	0.322
	79-501	8.46	9.71	7.37	45,900	34,800	3,970	1,810	2,710	0.3	0.241

*Not calculated, but assumed to be low temperature rod with fuel center temperature < disclocation release temperature.

†Measured gas release times $(\%\ TD/100)^{10.25}$, where TD = theoretical density.

**Calculated value not available.

TABLE 2 (Cont)

Rod Serial No.	Time In-Pile (1000 Hours)	Linear Power (KW/ft) Peak	Linear Power (KW/ft) Ave.	U + Th Burnup (MWD/MTM) Peak	U + Th Burnup (MWD/MTM) Ave.	Peak Fuel Temp. (°F) Center	Peak Fuel Temp. (°F) Surface	ThO_2 Disl'cn. Release Temp., T_d (°F)	Fission Gas Release (%) Measured	Fission Gas Release (%) Normalized†
C. $ThO_2 + U^{235}O_2$ Fuel (Cont)										
79-506	12.10	14.48	10.25	21,100	14,900	3,231	1,026	2,660	2.0	1.222
79-509	12.10	13.20	9.43	15,100	10,800	2,497	880	2,660	0.1	0.093
79-513	12.10	7.19	5.48	9,200	7,000	1,440	775	2,660	<0.1	0.032
79-514	12.10	7.19	5.48	9,200	7,000	1,440	775	2,660	<0.1	0.025
79-522	12.10	11.74	7.95	13,100	8,900	2,028	804	2,660	0.2	0.166
79-551	3.26	16.37	16.37	8,500	8,500	3,629	816	2,780	0.9	0.520
79-570	5.90	14.03	10.14	7,800	5,600	2,466	804	2,720	0.1	0.080
79-592	14.40	14.23	9.82	17,200	11,900	2,554	914	2,645	0.1	0.116
79-573	5.90	13.64	9.63	7,800	5,600	3,160	1,044	2,720	1.8	0.828
79-575	16.90	16.40	12.33	26,000	19,500	3,240	820	2,625	1.3	1.014
79-576	10.20	13.88	10.46	28,200	21,300	2,860	1,060	2,670	0.4	0.308
79-586	14.40	13.79	9.85	18,200	13,000	3,235	1,159	2,645	1.0	0.475
79-588	6.90	5.80	5.80	24,300	24,300	2,908	1,493	2,705	0.2	0.150
79-590	6.90	6.00	6.00	25,200	25,200	2,908	1,493	2,705	0.2	0.175
79-591	6.90	6.10	6.10	25,700	25,700	2,908	1,493	2,705	0.2	0.166
79-602	0.70	11.74	9.39	4,300	3,500	3,410	1,250	2,930	0.1	0.069
79-603	0.70	11.46	9.17	4,400	3,500	4,260	1,560	2,930	0.3	0.187
79-605	14.50	10.86	8.23	55,400	42,000	3,780	1,570	2,640	1.1	0.756
79-608	14.50	11.13	9.11	56,500	46,200	3,240	1,310	2,640	1.1	0.848
79-610	3.65	8.24	4.81	10,400	6,100	2,980	1,520	2,770	0.1	0.060
79-613	5.90	9.69	5.86	18,800	11,400	3,070	1,475	2,720	0.2	0.119
79-617	5.90	9.05	5.39	20,500	12,200	3,010	1,600	2,720	0.1	0.075
79-623	5.90	9.55	5.65	21,300	12,600	2,915	1,455	2,720	0.1	0.082
79-631	3.34	8.28	5.03	10,900	6,500	2,470	1,335	2,780	0.1	0.081
79-632	3.34	8.56	5.14	10,900	6,500	2,655	1,430	2,780	0.1	0.073
79-656	19.70	7.27	7.27	48,900	48,900	**	**	**	0.2	0.164
79-671	10.50	7.34	7.34	28,600	28,600	2,325	1,310	2,665	0.3	0.220

**Calculated value not available.

†Measured gas release times $(\%\ TD/100)^{10.25}$, where TD = theoretical density.

TABLE 3. SUMMARY OF IRRADIATED FUEL ROD HELIUM RECOVERY MEASUREMENTS

Rod Serial No.	Helium Recovery (%)	Comments
81-39	84.0	
81-46*	60.0	Low helium recovery
81-53	92.0	
81-74	117.0	
81-76	107.0	
81-81	94.0	
81-85	91.0	
79-318	124.0	Helium overpressure possible
79-320	75.0	
79-349	85.7	
79-363	98.0	
79-382	85.0	
79-429	87.5	
79-439	88.0	
79-442	96.5	
79-445*	36.0	Low helium recovery
79-449	107.0	
79-455	87.0	
79-467	95.5	
79-477*	157.0	High helium recovery
79-478	102.0	
79-481	105.0	
79-500	138.0	Helium overpressure possible
79-501	203.0	Helium overpressure possible
79-506	107.0	
79-509	105.2	
79-513	100.4	
79-514	97.7	
79-522	99.2	
79-551	95.2	
79-570	89.0	
79-572	90.0	
79-573	105.0	
79-575	91.0	
79-576	83.0	

*Gas release questionable because of exceptionally low or high helium recovery.

TABLE 3 (Cont)

Rod Serial No.	Helium Recovery (%)	Comments
79-586	122.0	Helium overpressure possible
79-588	105.1	
79-590	93.3	
79-591	117.0	
79-602	120.0	Helium overpressure possible
79-603	120.0	Helium overpressure possible
79-605	113.0	
79-608	116.0	
79-610	96.8	
79-613	97.1	
79-617	96.0	
79-623	93.8	
79-631	91.5	
79-632	107.0	
79-656	132.0	Helium overpressure possible
79-671*	160.0	High helium recovery

*Gas release questionable because of high helium pressure.

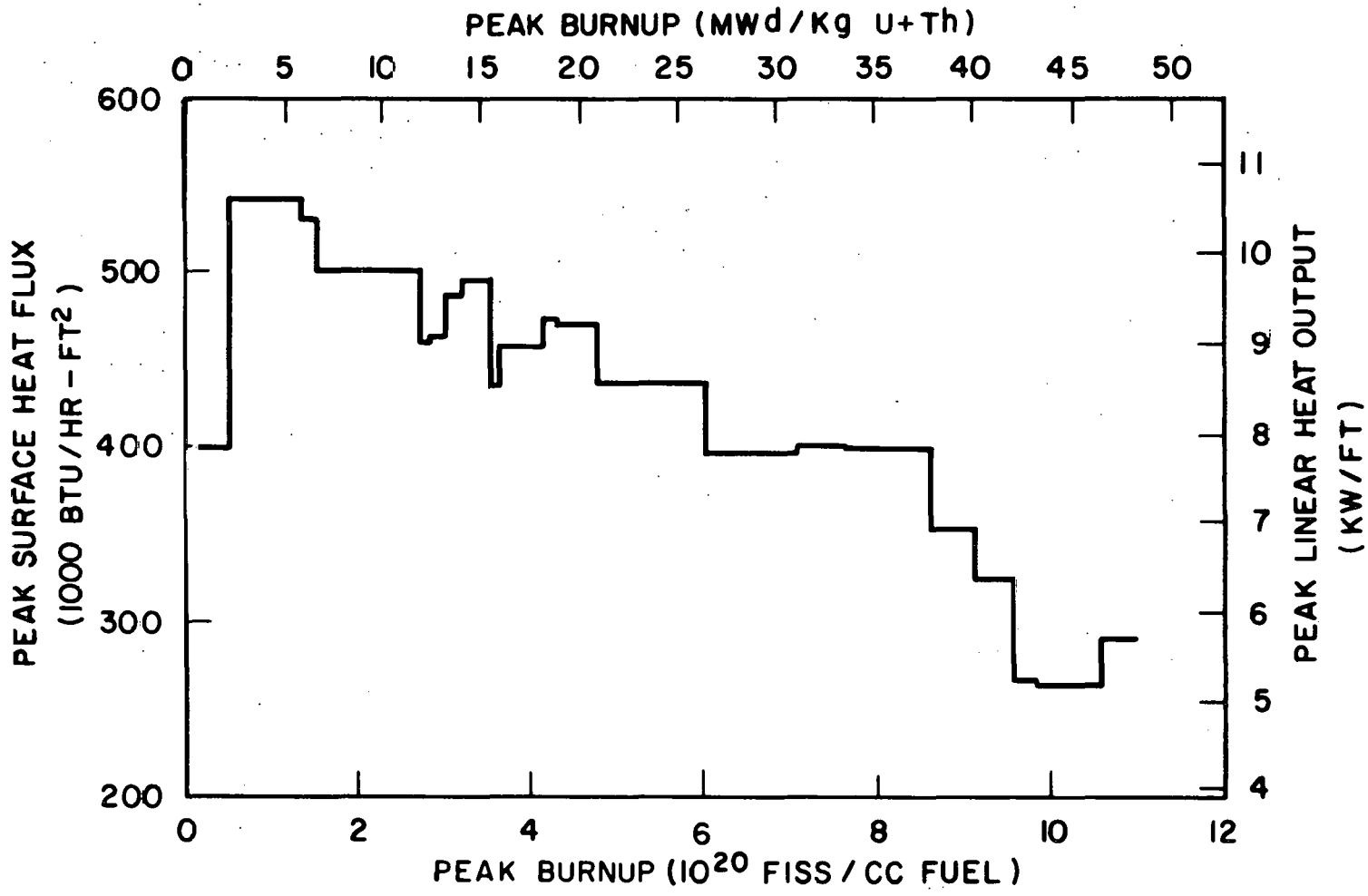

Figure 1. Rod 79-442 Peak Power-Burnup History

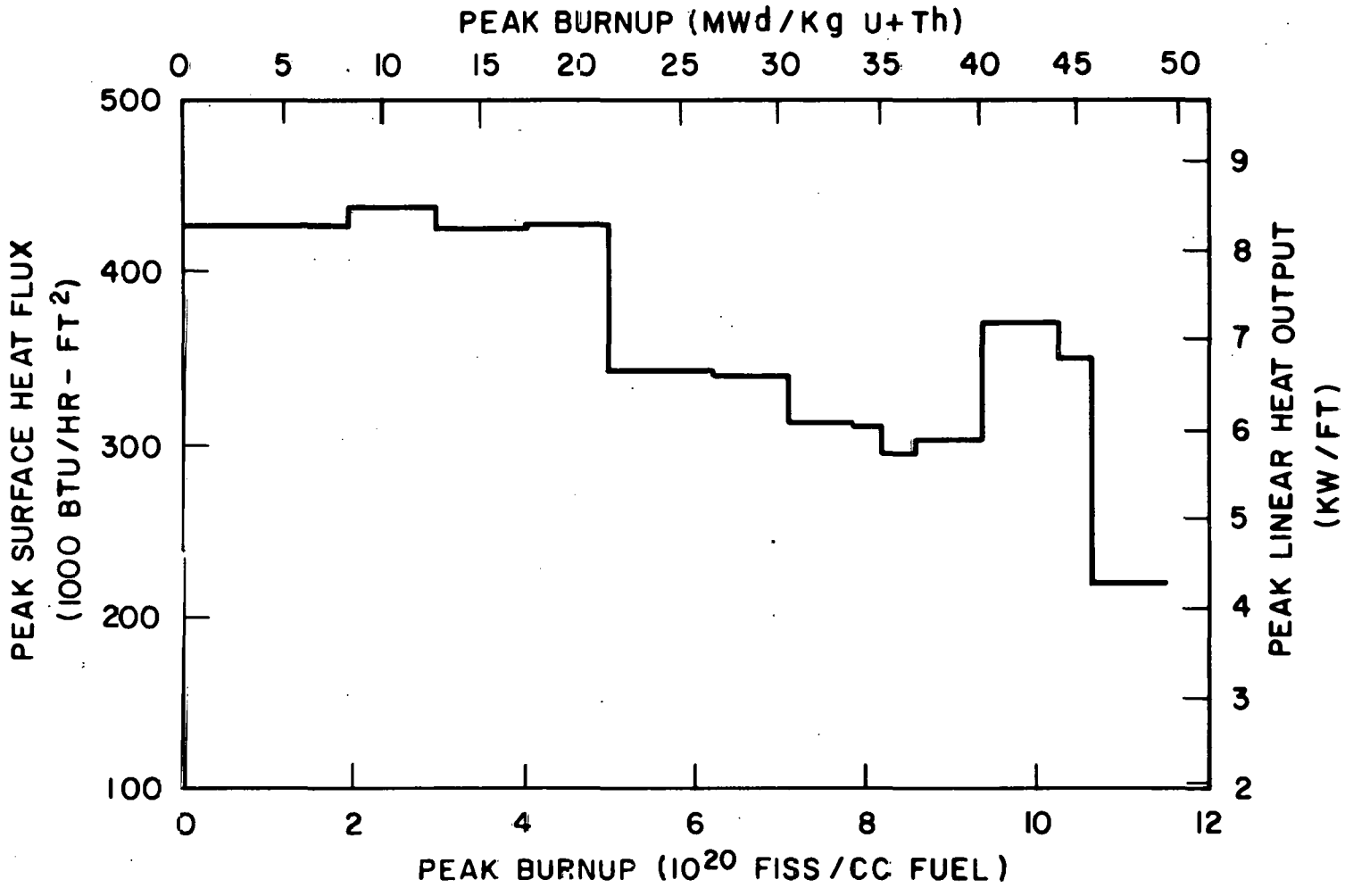

Figure 2. Rod 79-481 Peak Power-Burnup History

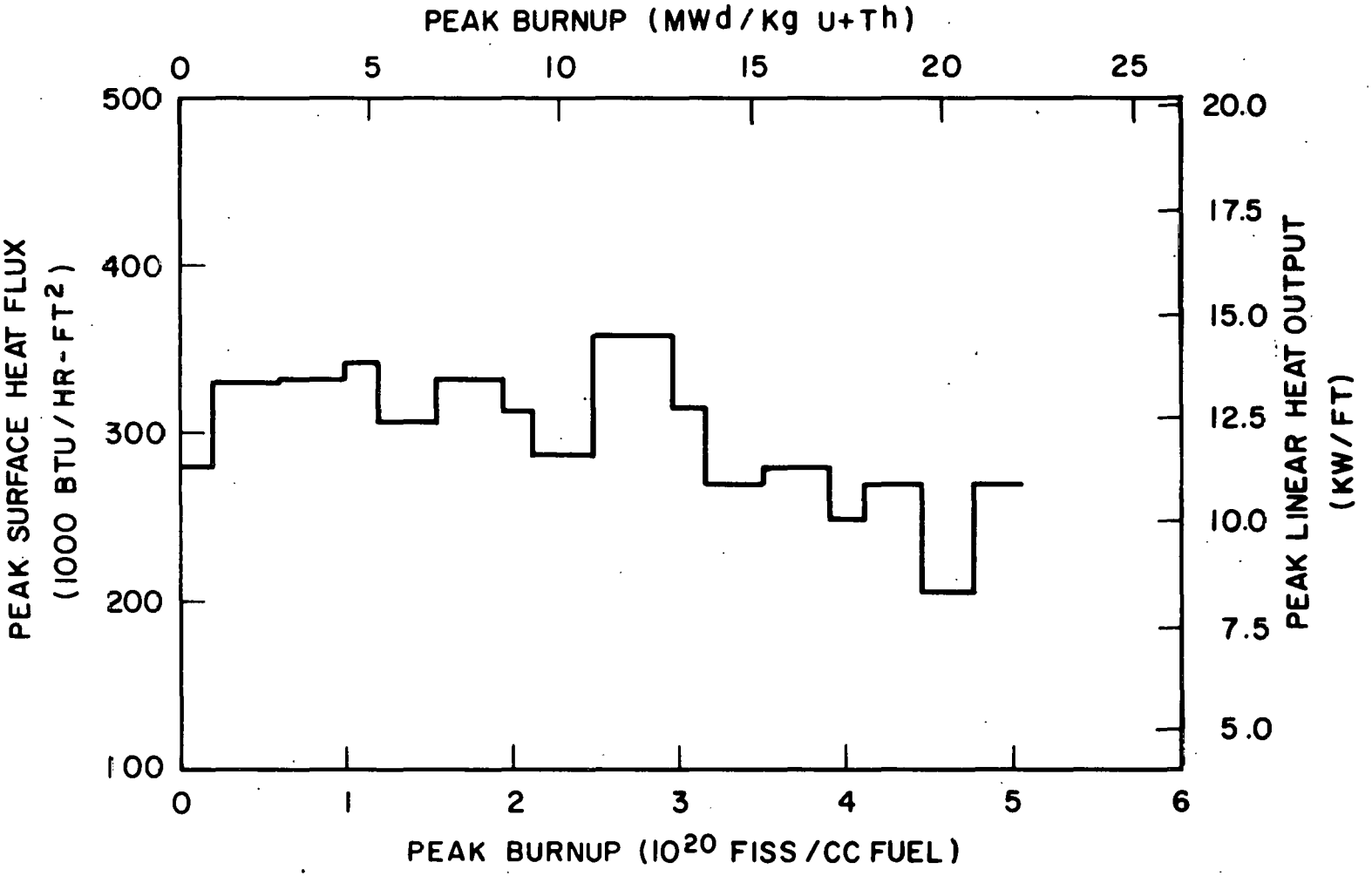

Figure 3. Rod 79-506 Peak Power-Burnup History

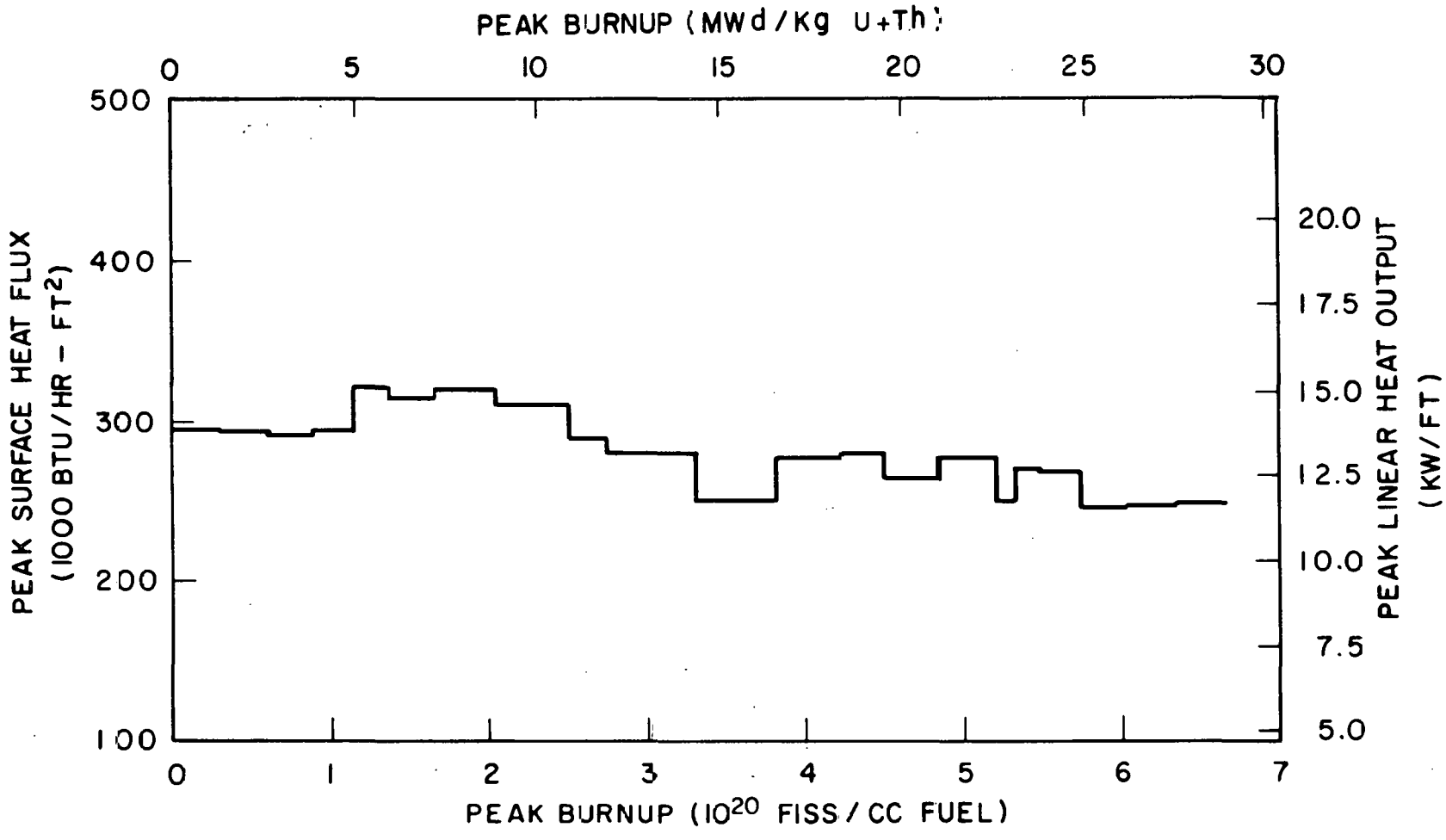

Figure 4. Rod 79-576 Peak Power-Burnup History

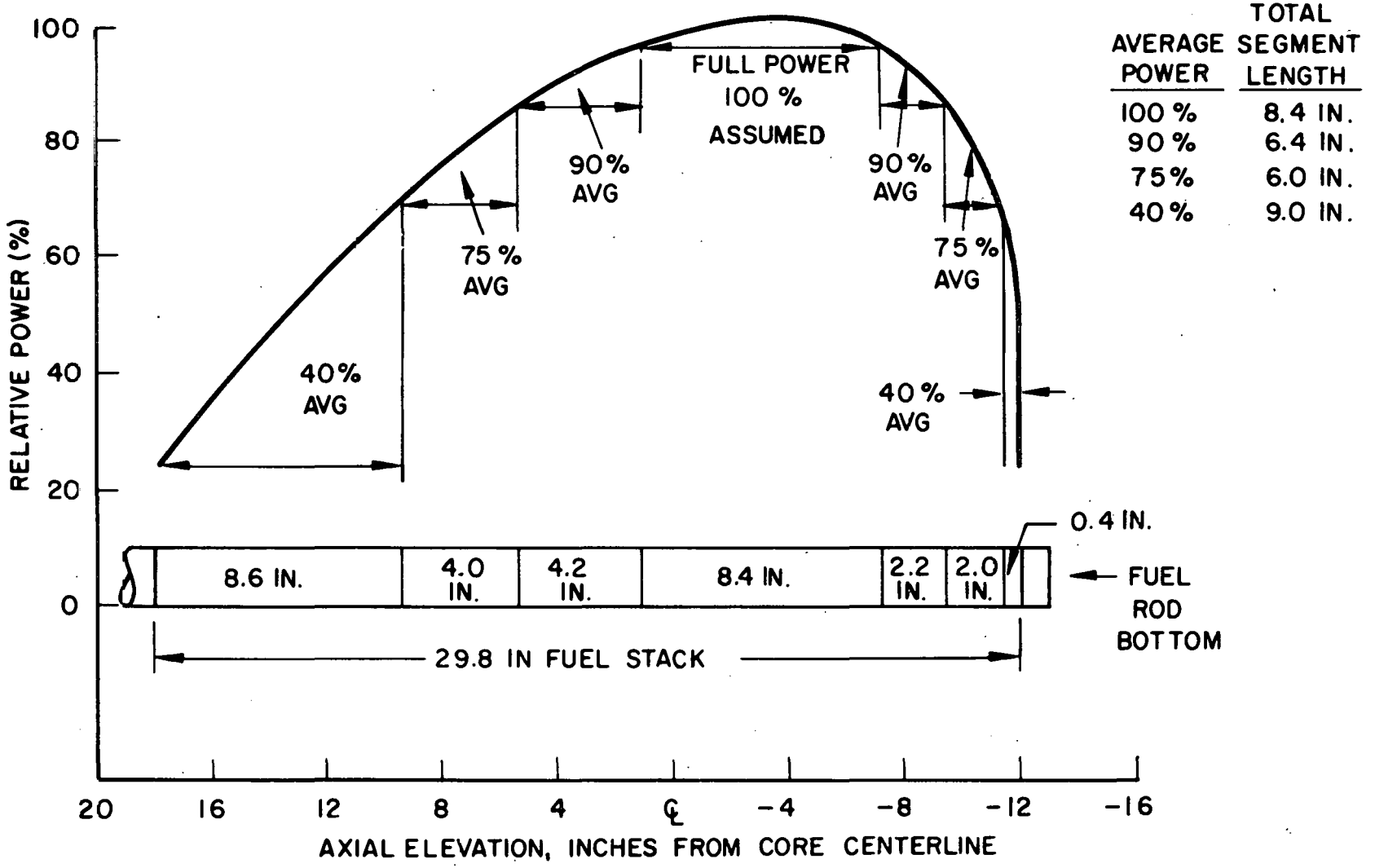

Figure 5. Schematic of Average Power Segments at Constant Temperature: Sample Rod 79-573

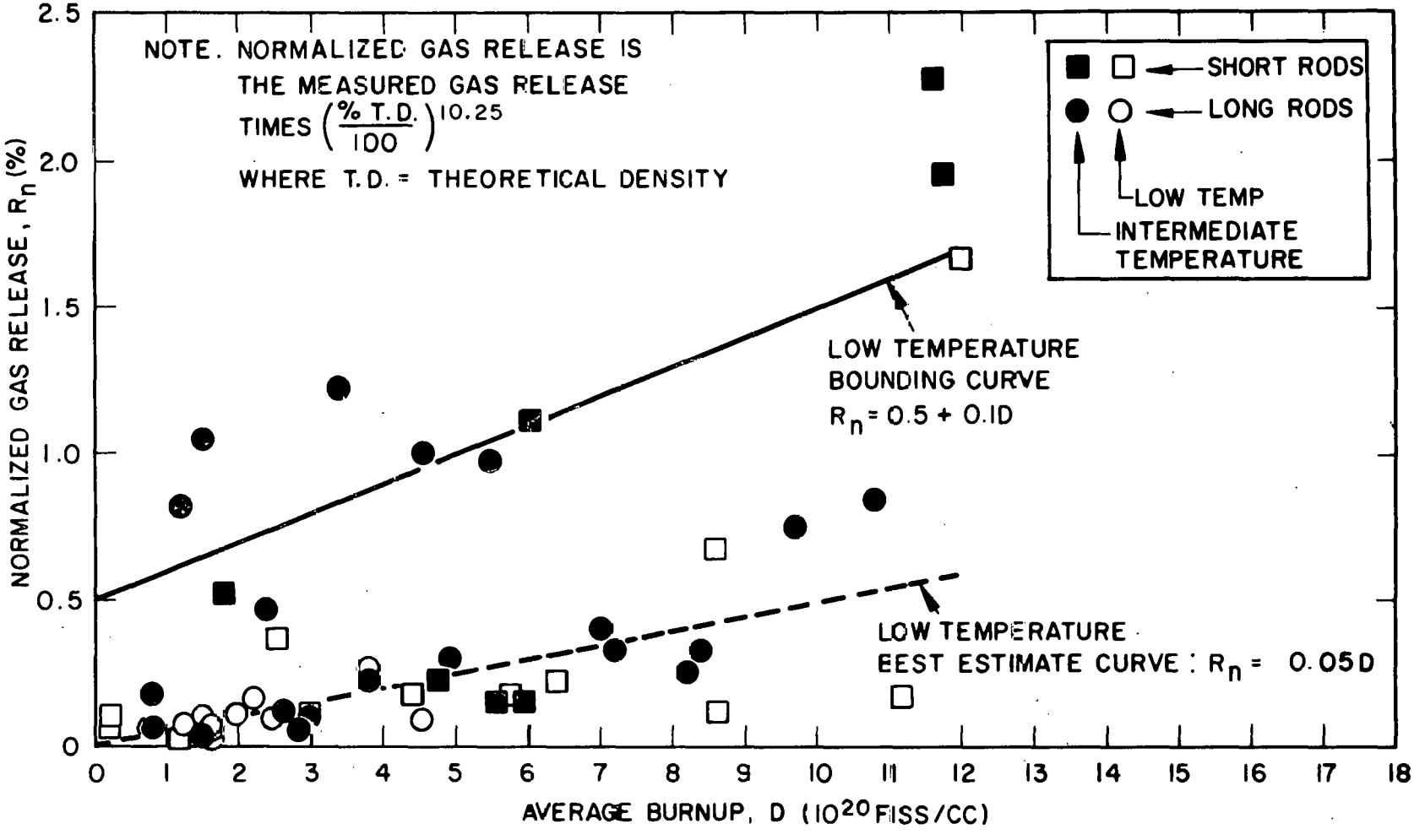

Figure 6. Normalized Gas Release Measured Versus Average Rod Burnup for LWBR Irradiation Test Rods

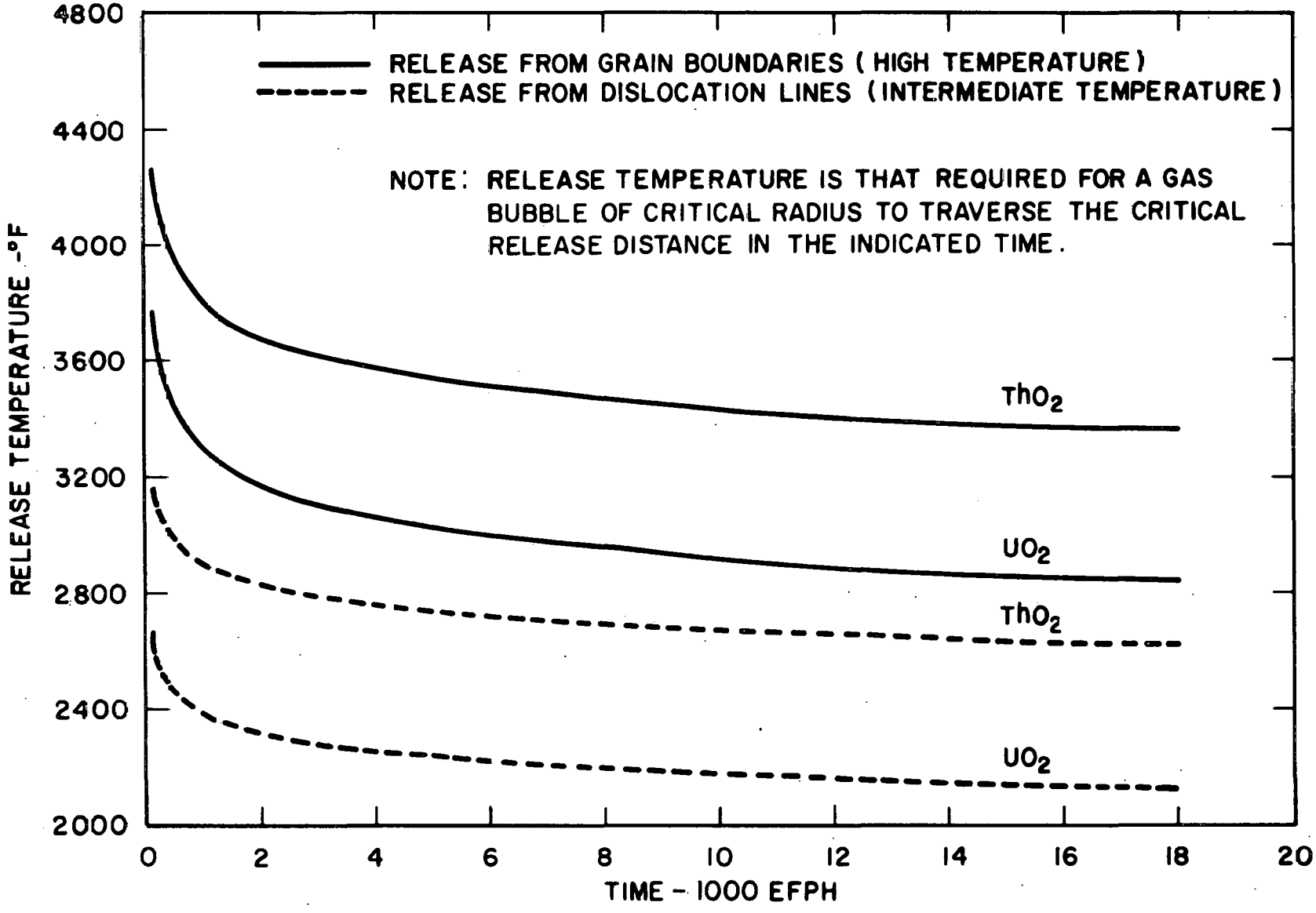

Figure 7. Bubble Release Temperatures

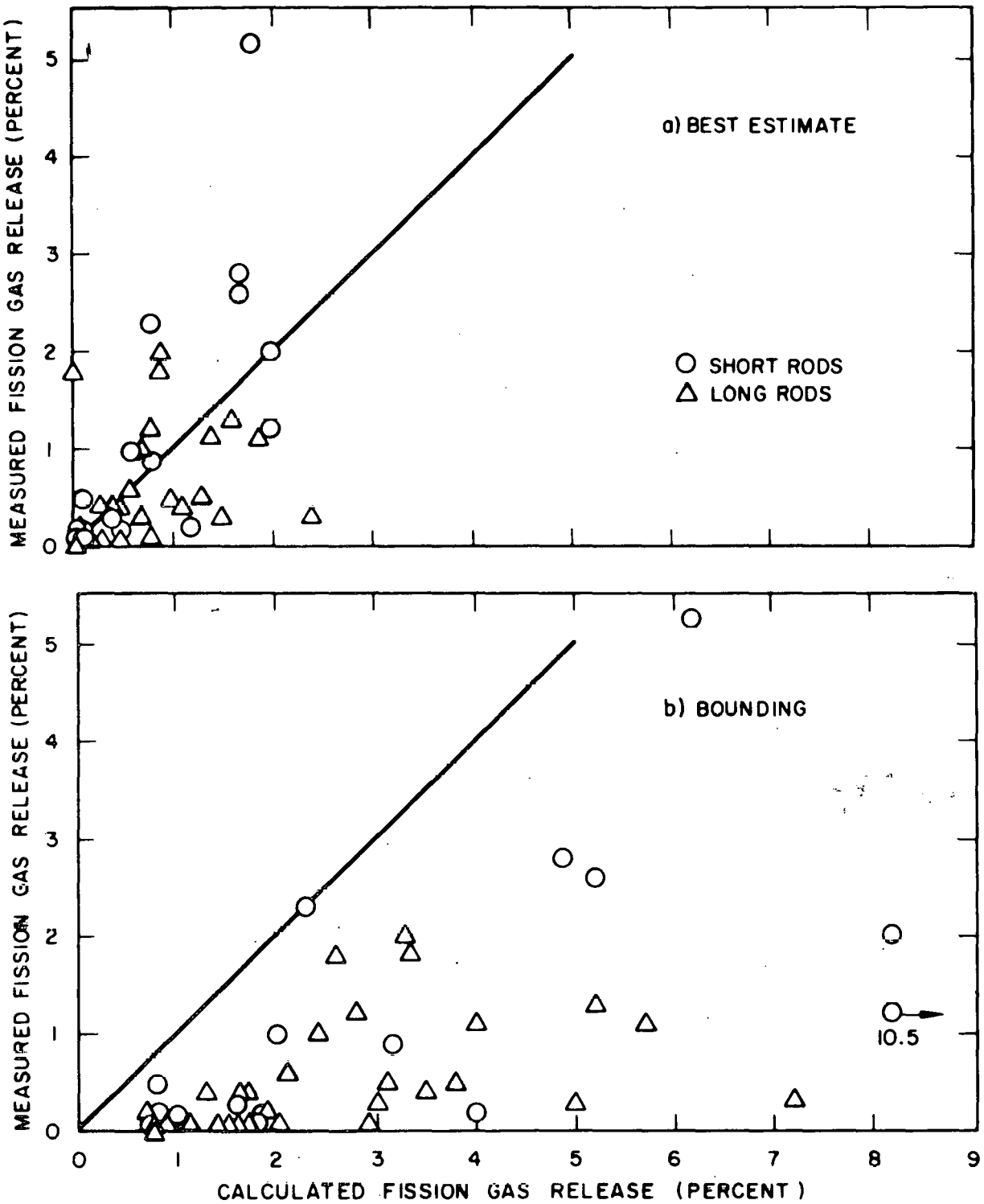

Figure 8. Comparison of Measured to Calculated Fission Gas Release from ThO_2 and ThO_2-UO_2 Fuel

*U.S. GOVERNMENT PRINTING OFFICE: 1978-703-115/864